ELSEVIER

Journal of Materials Processing Technology 112 (2001) 29–36

Journal of Materials Processing Technology

www.elsevier.com/locate/jmatprotec

Effects of profile shifted factor and pressure angle on the ZK-type dual-lead worm gear drives

Biing-Wen Bair[a,*], Chung-Biau Tsay[b]

[a]Department of Mechanical Engineering, National Lien Ho College of Technology and Commerce, Miao Li 36012, Taiwan, ROC
[b]Department of Mechanical Engineering, National Chiao Tung University, Hsinchu 30050, Taiwan, ROC

Received 5 May 2000; accepted 24 September 2000

Abstract

In the light of a mathematical model of the ZK-type dual-lead worm gear set proposed in the authors' recent work, this study adopts tooth contact analysis to compute the kinematic errors, instantaneous contact teeth (ICT) and average contact ratios (ACR). An elastic deformation of 3 μm is allowed while calculating ICT and ACR. In addition, increasing the ICT from three to four or from four to five reduces the root stress of the gear set due to its multiple contact teeth. Although a worm gear driven with a small pressure angle can increase the ICT, a worm gear with a small pressure angle incurs a more serious undercutting phenomena. Undercutting can also be averted by applying a positive-shifted modification of the hob cutter during the worm gear generation. Moreover, the boundary of conjugate and non-conjugate surface regions appears on the worm gear tooth surface when the worm gear has a low pressure angle. The non-conjugate region also influences the transmission efficiency, operational life time and noise of the worm gear drive. Furthermore, worm gear generation with a negative-shifted modification can decrease the unfavorable non-conjugate region.

Keywords: Undercutting; Instantaneous contact teeth; Average contact ratio

1. Introduction

For gear manufacturing, a hob cutter with standard axial module and widely commercialized teeth number is generally chosen to reduce the manufacturing cost. To fulfill the specified center distance and gear ratio, gear tooth surface is cut by shifting the hob cutter from standard pitch radius. The generated profiles-shifted gear has a modified addendum, contact ratio, gear root stress and tooth thickness. In addition, undercutting and addendum radius limit the amount of shifted-modification between hob cutter and generated gear.

Four forms of double developing worm gear drives [1] are typically used: (1) Hindley worms; (2) helical gears and their enveloping worms; (3) Lorentz worms; and (4) plane toothed wheels and their enveloping worms. The contact ratio and loading capacity of double enveloping worm gear drives exceed those of the single enveloping worm gear drives. Therefore, the double enveloping worm gear drive, which belongs to high-contact-ratio gear drives, is applied to the transmission mechanisms of heavy-load machines. However, the manufacturing cost and undercutting phenomena are two major limitations of the double enveloping worm which prevent industrial application.

Five single enveloping worm gear drives: ZA, ZN, ZI, ZK and Flender types are conventionally used. The characteristics of single enveloping worm gear drives have received extensive attention [2–7]. According to these investigations, the tooth addendum, pressure angle, tooth size and center distance variations can influence the contact ratio of the gear set. In addition, a worm gear drive with a large axial module and small pressure angle may increase its instantaneous contact teeth (ICT) and average contact ratio (ACR). Therefore, a single enveloping worm gear drive with a small pressure angle may replace the double enveloping worm gear drive in heavy-load machine applications. Undercutting occurs when the worm gear set has a large axial module or a lower pressure angle. Litvin [8] mathematically analyzed the undercutting conditions. The undercutting line on the generated worm gear surface can be averted by using non-orthogonal worm gears with cylindrical worms. Meshing conditions are quite favorable in terms of lubricant supply conditions. When the gear tooth has two parameter-family surfaces, two equations of meshing are available for the gear set. Although proposing the undercutting conditions with two parameters, Litvin et al. [9] did not analyze how to avert

* Corresponding author. Tel.: +886-3732-3152.
E-mail address: bairwen@oldmail.lctc.edu.tw (B.-W. Bair).

0924-0136/01/$ – see front matter
PII: S0924-0136(00)00848-7

the undercutting under a small pressure angle and/or a large module. Kuang and Yang [10] applied a semi-empirical equation to evaluate the fillet stress concentration for gears cut by a profile-shifted cutter. Gear tooth surfaces cut by a positive-shifted cutter can improve the undercutting phenomena.

The ZK-type dual-lead worm can be generated by a disk-type grinding wheel. However, the generated worm surfaces may have surface deviations, attributed primarily to manufacturing, heat treatment and cutter-tool profile errors. Nevertheless, sensitivity analysis can be performed to obtain the corrective machine-tool settings and optimal cutter profile modifications. Therefore, regrinding the worm on the basis of sensitivity analysis results, enables the minimizing of the surface deviations of a worm gear drive. Owing to the two different axial modules of a dual-lead worm, the worm thickness is varied for each worm tooth; the backlash is decreased along the worm's axial direction also. To increase the contact ratio, a worm gear drive with a low pressure angle is chosen to increase the ICT. Further, dual-lead worm gear drives with low pressure angles are used for machines to operate without or to minimize backlash and can absorb impact forces. When a low pressure angle is adopted for worm gear drives, a boundary line of conjugate and non-conjugate regions may exist on the worm gear surface. However, the shifted amount of the cutters also influences the boundary line of conjugate and non-conjugate regions.

The worm gear tooth surfaces may have conjugate and non-conjugate regions. Further, gear teeth undercutting may also occur. Interestingly, the friction for gear tooth surfaces varies during the meshing process. The favorable working region of the worm gear drive is its conjugate regions without undercutting. In addition, a worm gear drive with multiple contacts can increase the ICT, subsequently reducing the contact stress of the gear tooth surfaces. In practice, the ICT and ACR of a worm gear drive can be increased by selecting a low pressure angle, a large module, a large addendum and a shifted-cut gear tooth profile. In the light of above developments, this study investigates not only the undercutting phenomena and the boundary line of conjugate and non-conjugate regions, but also how hob cutter shifted modification influences the worm gear drive.

2. Boundary line of conjugate and non-conjugate regions

This work uses the mathematical model of the ZK-type dual-lead worm gear drive proposed in the authors' recent work [11,12]. Fig. 1 illustrates the coordinates relation between the generated worm gear and dual-lead worm-type hob cutter. Parameter A_4 represents the amount of hob cutter shifted modification, which equals the coefficient of worm gear modification which multiplies the nominal axial module. A positive sign of A_4 represents a positive-shifted cut of

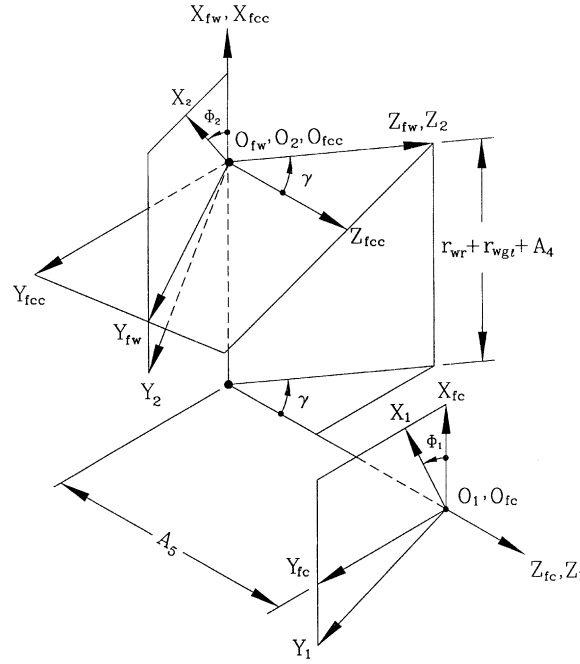

Fig. 1. Coordinate systems between a dual-lead worm-type hob cutter and the generated worm gear.

the worm gear and produces a worm gear with a lower undercutting line. In addition, the amount of shifted-modification influences the boundary line of the conjugate and non-conjugate regions.

A boundary line of the conjugate and non-conjugate regions always exists on the worm gear tooth surfaces. In addition, the equation of meshing between the generated worm gear and the hob cutter has no solution in the non-conjugate region. Therefore, an undercutting line may occur on the conjugate region of a worm gear tooth surface when a low pressure angle and/or a large axial module are adopted. Interestingly, the gear drive conjugate and non-conjugate distribution areas influence the transmission efficiency and load capacity. To improve the transmission conditions, the non-conjugate region on worm gear surfaces must be minimized to avert the undesired meshing.

The equation of meshing of the hob cutter left-side surface and worm gear right-side surface is given as follows [11]:

$$\sin(\phi_1 - \varphi + \delta) = \frac{-L_1}{\sqrt{M_1^2 + N_1^2}}, \tag{1}$$

where

$$B_{1l} = (u\sin\alpha_r - b_r)\sin\beta_1 + u\cos\alpha_r\cos\beta_1\sin\theta,$$
$$C_{1l} = u\cos\alpha_r\cos\theta + (r_{gr} + r_{wl} + A_3),$$
$$D_{1l} = u\cos\alpha_r\sin\beta_1\sin\theta - (u\sin\alpha_r - b_r)\cos\beta_1 - A_2,$$
$$E_{1r} = \sin\alpha_r\cos\beta_1\sin\theta - \cos\alpha_r\sin\beta_1,$$
$$F_{1r} = \sin\alpha_r\cos\theta,$$
$$G_{1r} = \sin\beta_1\sin\alpha_r\sin\theta + \cos\beta_1\cos\alpha_r,$$

$$H_{1r} = r_{wgr} + r_{wl} + A_4,$$

$$L_1 = \{[F_{1r}(D_{1l} - P_l\varphi) - C_{1l}G_{1r}]\sin\gamma + H_{1r}E_{1r}\cos\gamma\}m_{21},$$

$$M_1 = \{[-E_{1r}(D_{1l} - P_l\varphi) + B_{1l}G_{1r}]\sin\gamma + H_{1r}F_{1r}\cos\gamma\}m_{21},$$

$$N_1 = (C_{1l}E_{1r} - B_{1l}F_{1r})(1 - m_{21}\cos\gamma) + m_{21}H_{1r}\sin\gamma\, G_{1r} + A_5 m_{21}\sin\gamma[-E_{1r}\sin(\phi_1 - \varphi) + F_{1r}\cos(\phi_1 - \varphi)],$$

$$\sin\delta = \frac{M_1}{\sqrt{M_1^2 + N_1^2}}.$$

According to Eq. (1), if the parameters satisfy: (a) $M_1^2 + N_1^2 > L_1^2$ then the corresponding worm gear surface is a conjugate region (i.e. the numerical solution of $\sin(\phi_1 - \varphi + \delta)$ is between -1 and 1); (b) $M_1^2 + N_1^2 < L_1^2$ the corresponding worm gear surface is a non-conjugate region (i.e. the numerical solution of $\sin(\phi_1 - \varphi + \delta)$ is either less than -1 or larger than 1); and (c) $M_1^2 + N_1^2 = L_1^2$ represents the boundary curve of conjugate and non-conjugate regions (i.e. the numerical solution of $\sin(\phi_1 - \varphi + \delta)$ is equal to -1 or 1).

Example 1. Some design parameters of the chosen dual-lead worm gear set and hob cutter are listed in Table 1. The shifted-modification equals the nominal axial module (i.e. 3 mm) by multiplying by the coefficient of modification. The boundary between the conjugate and non-conjugate regions of the worm gear surface is calculated by applying the equation $M_1^2 + N_1^2 = L_1^2$ at the section $Z = 0$. Table 2 presents the coordinates of the boundary points of the conjugate and non-conjugate regions on the worm gear right-side surface with hob cutter shifted modifications. The boundary point coordinates of a non-shifted cut (i.e. shifted-modification = 0.0) are $X = -106.203$ mm, $Y = 2.607$ mm, $Z = 0$ mm and $R = 106.235$ mm. Simulation results indicate that the X-coordinates and R (i.e. $\sqrt{X^2 + Y^2}$) of the boundary points increase under a large positive-shifted modification. This finding suggests that the conjugate region decreases when a large positive-shifted modification is selected.

Table 1
Parameters of dual-lead worm gear set and hob cutter

Parameters of dual-lead worm	
Axial module	Left-side tooth surface, 2.9395 mm Right-side tooth surface, 3.0034 mm
Nominal axial module	3 mm
Pressure angle	Left-side tooth surface, 11°15′ Right-side tooth surface, 11°18′
Pitch diameter	Left-side tooth surface, 54.356 mm Right-side tooth surface, 49.755 mm
Nominal pitch diameter	50 mm
Tip diameter	58.3 mm
Root diameter	40.0 mm
Number of threads	1
Grinding wheel diameter	120.0 mm
Parameters of dual-lead oversize hob cutter	
Increased oversize diameter	2.0 mm
Compensation angle	7′16.5″
Parameters of dual-lead worm gear	
Number of teeth	72
Outside diameter	224.3 mm

Table 2
Coordinates of boundary points of conjugate and non-conjugate regions on the worm gear surface with shifted-modifications of hob cutter (mm)

Shifted-modification	X	Y	Z	R^a
−3.0	−106.064	2.001	−0.002	106.083
−2.4	−106.075	2.120	−0.001	106.097
−1.8	−106.097	2.240	0.002	106.121
−1.2	−106.133	2.361	0.006	106.159
−0.6	−106.130	2.481	−0.000	106.159
0.0	−106.203	2.607	−0.000	106.235
0.6	−106.309	2.737	−0.000	106.344
1.2	−106.455	2.874	−0.000	106.494
1.8	−106.651	3.020	−0.000	106.694
2.4	−106.906	3.181	−0.001	106.954
3.0	−107.232	3.360	−0.001	107.285

[a] $R = \sqrt{X^2 + Y^2}$.

3. Undercutting

For a regular gear surface, each point on the gear surface has a tangent plane. Regular surfaces are designed for gear drives to operate smoothly during gear meshing. A surface point at which the tangent plane does not exist is called a singular point of the surface. A singular point occurring on the gear surface may incur weakness in the gear surface's strength and a mismatch in gear meshing. In related work, Fong and Tsay [13] applied the characteristics of the surface unit normal to calculate the undercutting of spiral bevel gears. Assuming that the position vector of a surface is denoted as $\mathbf{R}$ and its surface parameters are u and θ, then the tangent plane is composed of two vectors: $\partial\mathbf{R}/\partial u$ and $\partial\mathbf{R}/\partial\theta$. The surface normal $\mathbf{N}$ can be obtained from

$$\mathbf{N} = \frac{\partial\mathbf{R}}{\partial u}\frac{\partial\mathbf{R}}{\partial\theta}. \tag{2}$$

A singular point appears as long as at least one of the partial derivatives in Eq. (2) equal to zero. Based on the tangent plane or tangent (partial derivative) existence concept, a singular point on the worm gear's surface can be defined and calculated.

The mathematical model of the worm gear set is a complex model represented in implicit form. Therefore, singular points of the worm gear surface are calculated by applying the numerical method. To compute the singular points on the worm gear surface, the calculated procedure can be simplified as a two-dimensional problem. The worm gear surface is cut into many cross-sections perpendicular to the axis of the worm gear rotation (i.e. the Z-direction). Then, the singular point on each worm gear's cross-section curve can be investigated by confirming the singularity of

Table 3
Coordinates of undercutting points on the worm gear surface (at cross-section $Z = 0$ mm) with various shifted-modifications of hob cutter (mm)

Shifted modification	X	Y	Z	R[a]
−3.0	−106.014	1.998	0.000	106.033
−2.4	−106.009	2.116	0.000	106.030
−1.8	−106.004	2.235	0.000	106.028
−1.2	−106.000	2.353	0.000	106.026
−0.6	−105.997	2.471	0.000	106.025
0.0	−105.993	2.590	0.000	106.025
0.6	−105.990	2.708	0.000	106.025
1.2	−105.988	2.827	0.000	106.025
1.8	−105.985	2.946	0.000	106.026
2.4	−105.983	3.064	0.000	106.027
3.0	−105.981	3.183	0.000	106.029

[a] $R = \sqrt{X^2 + Y^2}$.

each cross-section curve. If the tangent vector to the curve equals zero, then a singular point obviously exists. Each cross-section along the Z-direction is assigned a corresponding value to the Z-component of the worm gear mathematical model. The singular point on this corresponding cross-section curve is also calculated. The undercutting line can be obtained as the total singular points of each Z cross-section.

Example 2. The same worm gear set as that of Example 1 is adopted herein for undercutting analysis. By applying the above calculation procedures, the undercutting points of right-side surface of a worm gear with shifted modification of the hob cutter in section $Z = 0$ mm are shown in Table 3. The coordinates of the undercutting point under non-shifted modification at the cross-section $Z = 0$ mm are $X = -105.993$ mm, $Y = 2.590$ mm, and $R = 106.025$ mm, respectively. Applying a positive-shifted modification implies a decrease of the undercutting on X-coordinate. This find implies that X-coordinates of the undercutting points decrease under a large positive-shifted modification, and the conjugate region of the worm gear increases.

4. Contact teeth, kinematic errors and contact ratios

Fig. 2 depicts the coordinate system relationship between the worm and the worm gear. Owing to the tangency of two contacting gear tooth surfaces, the position vectors and unit normals of the worm and worm gear tooth surfaces, represented in coordinate system S_f, should be the same at the point of contact. Therefore, the following equations must be observed [14,15]:

$$\mathbf{R}_f^{(w)} = \mathbf{R}_f^{(g)}, \tag{3}$$

$$\mathbf{n}_f^{(w)} = \mathbf{n}_f^{(g)}. \tag{4}$$

Eq. (3) indicates that the position vectors of worm surface $\mathbf{R}_f^{(w)}$ and worm gear surfaces $\mathbf{R}_f^{(g)}$ have a common contact point. Three independent equations are to be utilized. Eq. (4)

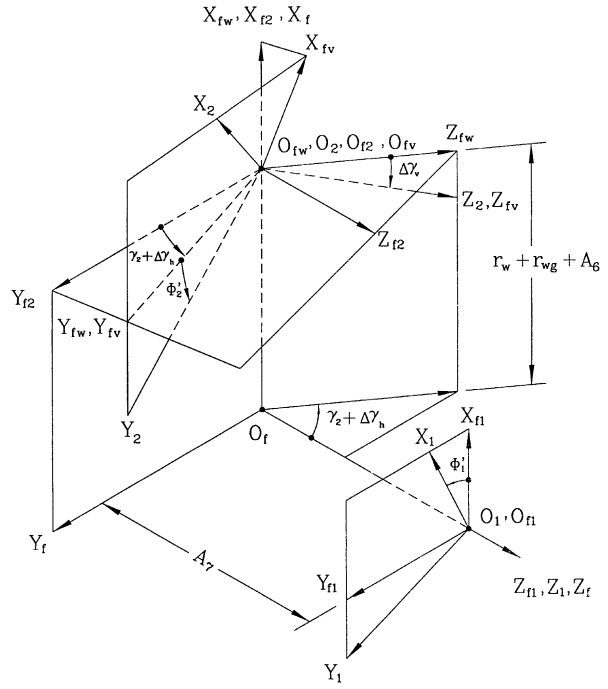

Fig. 2. Coordinate systems between a dual-lead worm-type worm gear.

indicates that the worm and worm gear tooth surfaces have a common surface unit normal at their common contact point. Eq. (4) possesses two independent equations since $|\mathbf{n}_f^{(w)}| = |\mathbf{n}_f^{(g)}| = 1$. In addition, two equations of meshing, i.e. the grinding wheel which generates the worm and the hob cutter which generates the worm gear, are two additional independent equations. Therefore, there are seven equations with eight parameters. Hence, the contact analysis computational procedure is based on the solution of a system of seven independent equations with eight unknowns: $u, \theta', \varphi', \phi_1', \theta, \varphi, \phi_1$ and ϕ_2', where θ' and φ' denote the surface parameters of the grinding wheel for worm surface generation, and φ and ϕ_1 represent the surface parameters of the hob cutter for worm gear generation. Based on the equations of meshing, parameter u can be expressed as an explicit function of θ: φ and ϕ_1 are also related. The worm gear rotation angle ϕ_2' depends on the worm rotation angle ϕ_1' during the gear set meshing process. In addition, parameter ϕ_1 is the hob cutter surface parameter. Since the worm is always a driving gear, the worm rotation angle ϕ_1' is considered a given value. Therefore, seven unknown parameters $u, \theta', \theta, \varphi, \varphi', \phi_1$ and ϕ_2' are solved with the seven equations. These seven equations are non-linear equations and can be solved by applying the Newton–Raphson numerical algorithm. The kinematic error of the gear set can be calculated by using the following equation [14,15]:

$$\Delta\phi_2'(\phi_1') = \phi_2'(\phi_1') - \frac{Z_1}{Z_2}\phi_1' \tag{5}$$

where Z_1 and Z_2 denote the tooth numbers and ϕ_1' and ϕ_2' represent the rotation angles of the worm and worm gear, respectively.

The contact ratio of a gear set is generally defined as its rotation angle, measured from the starting contact point to the end contact point, and divided by the angle formed by every two teeth [16]. The ICT for spur, helical, spiral bevel, and hypoid gears is always one or two teeth, and can be defined on the basis of the kinematic error curves of the gear set. In general, when two kinematic error curves are coupled, then the ICT is two; otherwise, the ICT is one. The contact ratio is also calculated from the kinematic error curves. However, the ICT of a dual-lead worm gear set can have more than two, three or even four teeth. Therefore, the contact ratio defined according to the kinematic error curves is inappropriate. An alternative method is to apply the TCA method and obtain the ICT and contact ratios. In this study, the TCA method is initially applied to calculate the first contact point and the kinematic errors. Then, the gear set surface elastic deformation 3 μm is allowed to verify all the possible instantaneous contact points for worm and worm gear surfaces at every instant (i.e. computed point). The ICT can be determined by the ICT numbers of the gear set. The ACR is defined as the sum of the ICT of the selected contact instants (i.e. computed points), divided by the total number of selected contact instants within one driving cycle.

To simulate the gear set assembly errors, three parameters A_6, $\Delta\gamma_v$ and $\Delta\gamma_h$ are considered in the meshing process, where A_6 denotes the center distance deviation of the worm gear set, and $\Delta\gamma_v$ and $\Delta\gamma_h$ represent the intersected and crossed misaligned angles of the worm gear set, respectively. The fact that the worm and worm gear surfaces are considered in the rigid body motion (i.e. no deformation) accounts for the initial contacts. The TCA and kinematic errors are calculated while considering one-tooth contact. The ICT is also calculated by applying the TCA method and allowing 3 μm of gear surface elastic deformation, confirming how many worm teeth come in to contact with the mating worm gear at every computed point.

Example 3. The worm gear set is chosen in the same manner as that in Example 1. Three parameters of assembly errors are considered: $A_6 = -0.3$ mm, $\Delta\gamma_v = 0.0'$ and $\Delta\gamma_h = -3.0'$. Parameter A_4 is the shifted modification while the hob cutter cuts the worm gear. When the standard worm gear (i.e. $A_4 = 0$ mm) is meshing with the worm, the gear set contact teeth (CT) and kinematic errors (KE) under above assembly conditions are illustrated in Fig. 3. According to this figure, the gear set contact initiates at the worm rotation angle 495.18° and, at that moment (i.e. computed point), the ICT is four teeth. Contact is completed at the worm rotation angle of −772.49°. At that moment, the ICT is four teeth. The maximum kinematic error of the worm gear set is 0.167 arc-second. By considering the numbers of contact teeth within the line of action, the ACR is calculated by summing the ICT at each computed point and dividing by the total computed points in the effective contact path. Based on such a TCA calculation method, the ACR is obtained as 3.611, as shown in Table 4. The conventional method for contact ratio calculation is the calculation by the worm rotation angle, measured from the beginning of contact to the end (i.e. 1267.67°), divided by one revolution of the worm (i.e. 360°). Based on the conventional calculation method, the contact ratio is 3.521, as also indicated in this table.

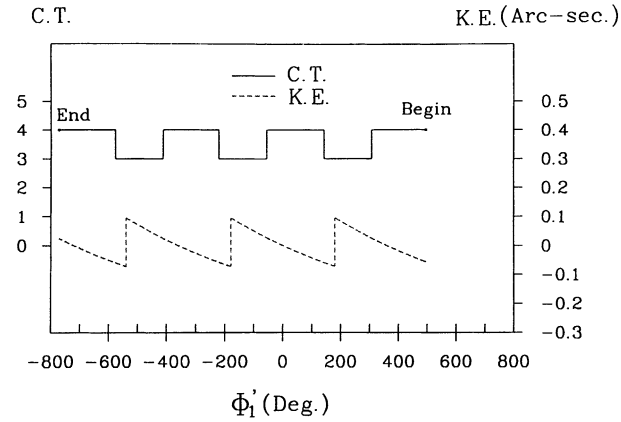

Fig. 3. Contact teeth and kinematic errors under assembly conditions: $A_4 = 0.0$ mm, $A_6 = -0.3$ mm, $\Delta\gamma_v = 0.0'$, $\Delta\gamma_h = -3.0'$.

When the worm gear is generated by hob cutters with a negatively shifted-modification, the contact teeth and kinematic errors of a worm gear drive with parameters $A_4 = -0.3$ and -0.6 mm are displayed in Figs. 4 and 5, respectively. Table 4 indicates that the ACR with parameter $A_4 = -0.3$ and -0.6 mm decrease to 3.594 and 3.589, respectively. The maximum kinematic error is reduced to 0.011 and 0.161 arc-seconds, respectively. According to the present results, the kinematic errors and the ACR of the worm gear set can be reduced with a negative-shifted cut.

Table 4
Kinematic errors and contact ratios under various assembly conditions (I)

Assembly conditions	Begin contact (degree)	End contact (degree)	ACR[a]	Contact ratio[b]	KE (arc-second)
$A_4 = 0.0$ mm, $A_6 = -0.3$ mm, $\Delta\gamma_v = 0.0'$, $\Delta\gamma_h = -3.0'$	495.18	−772.49	3.611	3.521	0.167
$A_4 = -0.3$ mm, $A_6 = -0.3$ mm, $\Delta\gamma_v = 0.0'$, $\Delta\gamma_h = -3.0'$	521.59	−739.47	3.594	3.503	0.011
$A_4 = -0.6$ mm, $A_6 = -0.3$ mm, $\Delta\gamma_v = 0.0'$, $\Delta\gamma_h = -3.0'$	548.00	−713.06	3.589	3.503	0.161
$A_4 = 0.3$ mm, $A_6 = -0.3$ mm, $\Delta\gamma_v = 0.0'$, $\Delta\gamma_h = -3.0'$	481.98	−798.90	3.646	3.558	0.331
$A_4 = 0.6$ mm, $A_6 = -0.3$ mm, $\Delta\gamma_v = 0.0'$, $\Delta\gamma_h = -3.0'$	468.77	−831.91	3.689	3.613	0.497

[a] ACR are determined based on the TCA computer simulations.
[b] Contact ratios are determined based on the worm in total contact rotation angle divided by 360°.

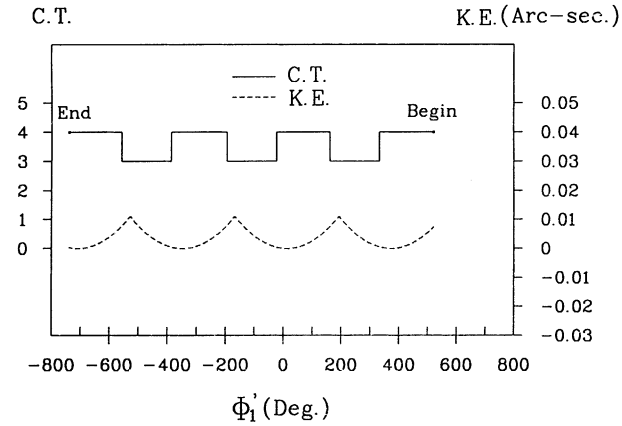

Fig. 4. Contact teeth and kinematic errors under assembly conditions: $A_4 = -0.3$ mm, $A_6 = -0.3$ mm, $\Delta\gamma_v = 0.0'$, $\Delta\gamma_h = -3.0'$.

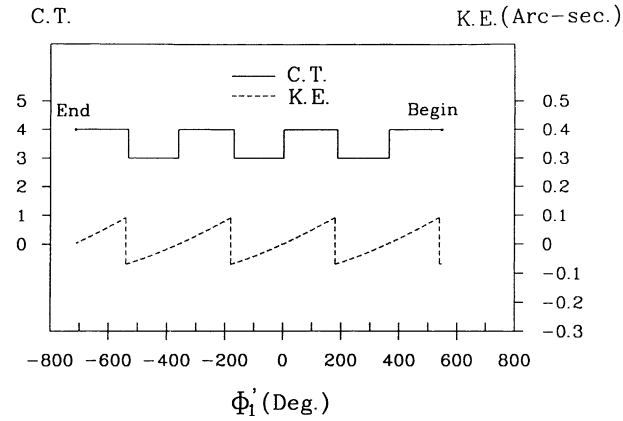

Fig. 5. Contact teeth and kinematic errors under assembly conditions: $A_4 = -0.6$ mm, $A_6 = -0.3$ mm, $\Delta\gamma_v = 0.0'$, $\Delta\gamma_h = -3.0'$.

Figs. 6 and 7 present the contact teeth and kinematic errors of a worm gear drive with positive-shifted parameters $A_4 = 0.3$ and 0.6 mm, respectively. Table 4 also indicates that the respective ACR increase to 3.646 and 3.689, and that

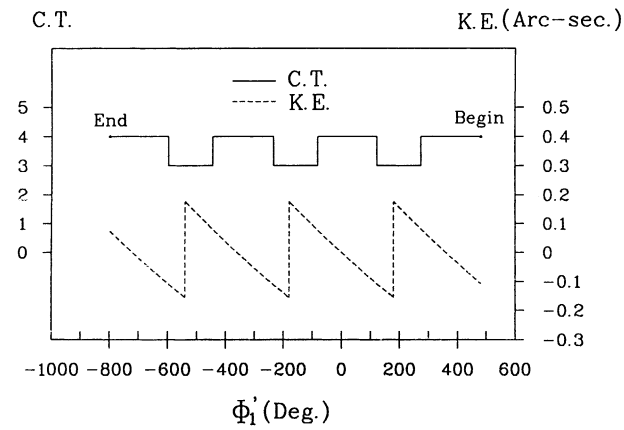

Fig. 6. Contact teeth and kinematic errors under assembly conditions: $A_4 = 0.3$ mm, $A_6 = -0.3$ mm, $\Delta\gamma_v = 0.0'$, $\Delta\gamma_h = -3.0'$.

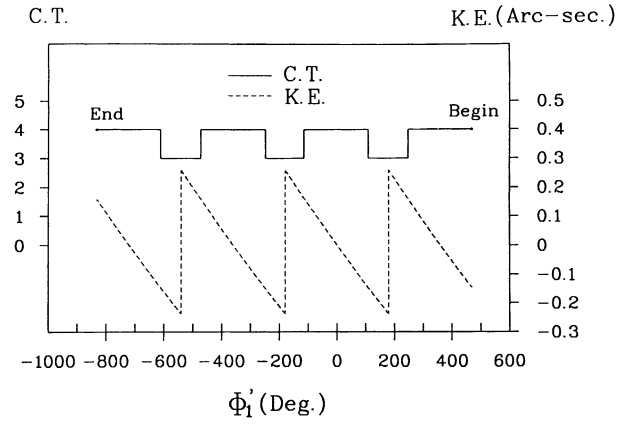

Fig. 7. Contact teeth and kinematic errors under assembly conditions: $A_4 = 0.6$ mm, $A_6 = -0.3$ mm, $\Delta\gamma_v = 0.0'$, $\Delta\gamma_h = -3.0'$.

the maximum kinematic errors increase to 0.331 and 0.497 arc-seconds, respectively. Simulation results indicate that the kinematic errors and ACR are increased with a positive-shifted cut.

Example 4. The same worm gear set as that of Example 1 is chosen except the pressure angles of the worm and hob cutter are changed to 9°. Fig. 8 illustrates the contact teeth and kinematic errors of the gear set under ideal assembly conditions. This figure indicates that the gear set contact initiates at a worm rotation angle of 587.62° and, at that instant, the ICT is five teeth. Contact is completed at a worm rotation angle of −858.32° and, at that instant, the ICT is also five teeth. According to Table 5, the maximum kinematic error of the worm gear set is 0.009 arc-second; and the ACR is increased to 4.041 also. When assembly errors occurred as $A_6 = -0.3$ mm, $\Delta\gamma_v = 0.0'$ and $\Delta\gamma_h = -3.0'$, the kinematic errors and contact teeth are shown in Fig. 9. The ACR is then decreased to 3.972 and the maximum error is increased to 0.157 arc-second, as indicated in Table 5. If the worm gear is generated by a hob cutter with

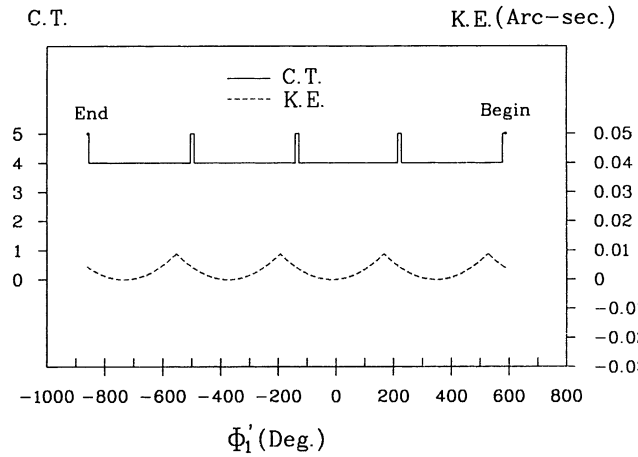

Fig. 8. Contact teeth and kinematic errors under ideal assembly conditions: $A_4 = 0.0$ mm, $A_6 = 0.0$ mm, $\Delta\gamma_v = 0.0'$, $\Delta\gamma_h = 0.0'$.

Table 5
Kinematic errors and contact ratios under various assembly conditions (II)

Assembly conditions	Begin contact (degree)	End contact (degree)	ACR[a]	Contact ratio[b]	KE (arc-second)
$A_4 = 0.0\,\text{mm}, A_6 = 0.0\,\text{mm}, \Delta\gamma_v = 0.0', \Delta\gamma_h = 0.0'$	587.62	−858.32	4.041	4.016	0.009
$A_4 = 0.0\,\text{mm}, A_6 = -0.3\,\text{mm}, \Delta\gamma_v = 0.0', \Delta\gamma_h = -3.0'$	567.81	−851.72	3.972	3.943	0.157
$A_4 = -0.3\,\text{mm}, A_6 = -0.3\,\text{mm}, \Delta\gamma_v = 0.0', \Delta\gamma_h = -3.0'$	607.43	−818.70	3.995	3.961	0.009
$A_4 = -0.6\,\text{mm}, A_6 = -0.3\,\text{mm}, \Delta\gamma_v = 0.0', \Delta\gamma_h = -3.0'$	653.64	−792.29	4.055	4.016	0.592
$A_4 = 0.3\,\text{mm}, A_6 = -0.3\,\text{mm}, \Delta\gamma_v = 0.0', \Delta\gamma_h = -3.0'$	534.80	−878.13	3.967	3.925	0.315
$A_4 = 0.6\,\text{mm}, A_6 = -0.3\,\text{mm}, \Delta\gamma_v = 0.0', \Delta\gamma_h = -3.0'$	508.39	−911.14	3.977	3.943	0.474

[a] ACR are determined based on the TCA computer simulations.
[b] Contact ratios are determined based on the worm in total contact rotation angle divided by 360°.

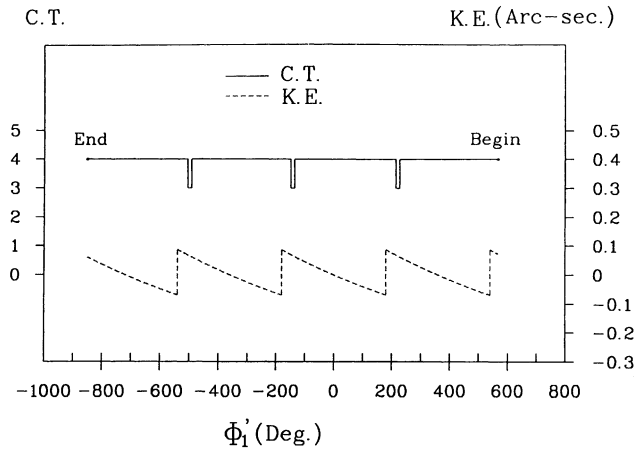

Fig. 9. Contact teeth and kinematic errors under assembly conditions: $A_4 = 0.0\,\text{mm}$, $A_6 = -0.3\,\text{mm}$, $\Delta\gamma_v = 0.0'$, $\Delta\gamma_h = -3.0'$.

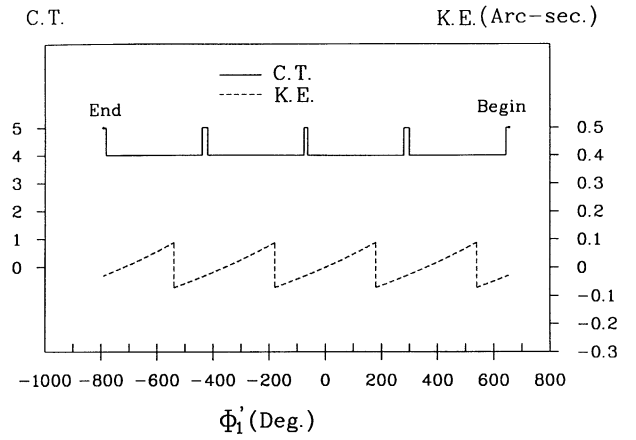

Fig. 11. Contact teeth and kinematic errors under assembly conditions: $A_4 = -0.6\,\text{mm}$, $A_6 = -0.3\,\text{mm}$, $\Delta\gamma_v = 0.0'$, $\Delta\gamma_h = -3.0'$.

a negative-shifted cut $A_4 = -0.3$ and -0.6 mm, the ACR is then increased to 3.995 and 4.055, respectively. Table 5 and Figs. 10 and 11 display the contact teeth and kinematic errors. The respective maximum kinematic errors are reduced to 0.009 arc-second and increased to 0.592 arc-second. The maximum ICT is four teeth and five teeth, respectively. When the worm gear is generated by hob cutters with a positive-shifted cut $A_4 = 0.3$ and 0.6 mm, then ACR is decreased to 3.967 and 3.977, respectively, as shown in Table 5 and Figs. 12 and 13. The respective maximum kinematic errors are increased to 0.315 and 0.474 arc-seconds. The above results confirm that a worm gear generated by hob cutters with a negative-shifted cut can increase the ACR, while a positive-shifted cut decreases the ACR. Moreover, the maximum kinematic error of the gear set may decrease with a negative-shifted cut.

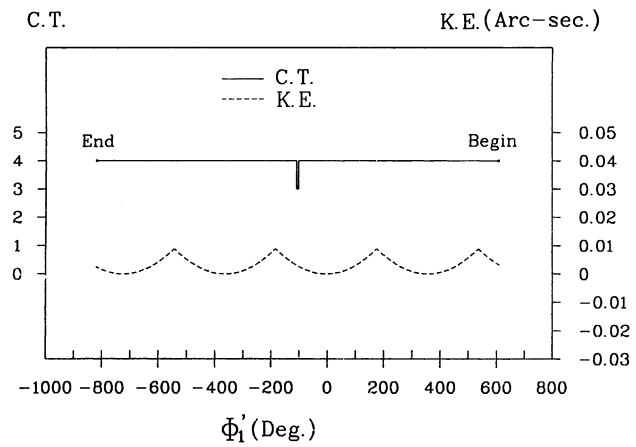

Fig. 10. Contact teeth and kinematic errors under assembly conditions: $A_4 = -0.3\,\text{mm}$, $A_6 = -0.3\,\text{mm}$, $\Delta\gamma_v = 0.0'$, $\Delta\gamma_h = -3.0'$.

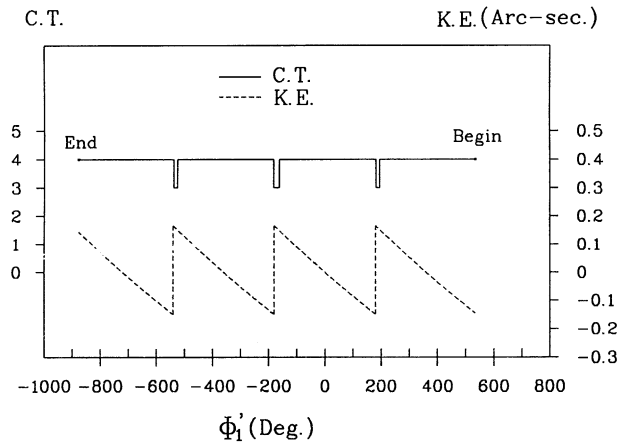

Fig. 12. Contact teeth and kinematic errors under assembly conditions: $A_4 = 0.3\,\text{mm}$, $A_6 = -0.3\,\text{mm}$, $\Delta\gamma_v = 0.0'$, $\Delta\gamma_h = -3.0'$.

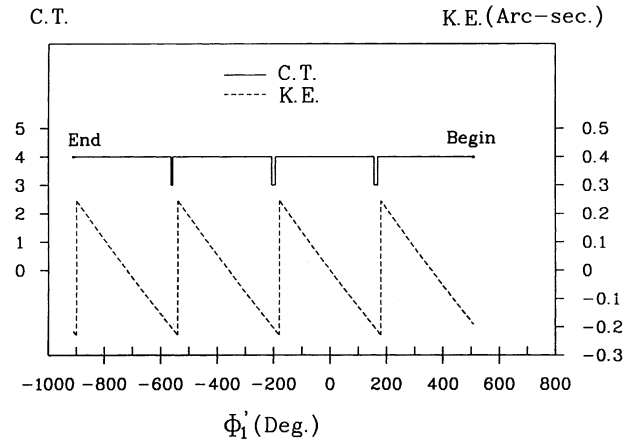

Fig. 13. Contact teeth and kinematic errors under assembly conditions: $A_4 = 0.6\,\text{mm}$, $A_6 = -0.3\,\text{mm}$, $\Delta\gamma_v = 0.0'$, $\Delta\gamma_h = -3.0'$.

5. Conclusions

A ZK-type dual-lead worm gear drive with a small pressure angle can increase the gear contact ratio and the ICT. At the same time the root stress of the gear set decreases due to its multiple contact teeth. However, a worm gear set with a small pressure angle may induce gear set undercutting and increase the gear's non-conjugate region. Gear undercutting can be averted by applying hob cutters with a positive-shifted cut. However, such an application increases the non-conjugate region and decreases the working area of the worm gear drive. If the worm gear is cut by hob cutters with a small pressure angle and with a proper shifted modification, the maximum root stress can decrease due to multiple contact teeth.

Acknowledgements

The authors would like to thank the National Science Council of the ROC for financially supporting a portion of this work under Contract No. NSC 84-2212-E009-016.

References

[1] K. Ishida, H. Ueda, S. Ohashi, Y. Fukui, Theoretical and experimental investigation of a new plane toothed wheel and its enveloping hourglass worm, ASME J. Mech. Des. 100 (1978) 460–469.
[2] T. Bercsey, P. Horák, A new tribological model of worm gear teeth contact, in: Proceedings of the Seventh International Power Transmission and Gearing Conference, DE-Vol. 88, 1996, pp. 147–152.
[3] S.I. Dudas, K. Banyai, G. Varga, Simulation of meshing of worm gearing, in: Proceedings of the Seventh International Power Transmission and Gearing Conference, DE-Vol. 88, 1996, pp. 141–146.
[4] H.S. Fang, C.B. Tsay, Mathematical model and bearing contacts of the ZK-type worm gear set cut by oversize hob cutters, J. Mechanism Mach. Theory 31 (3) (1996) 271–282.
[5] F.L. Litvin, I.H. Seol, Computerized determination of gear tooth surface as envelope to two parameter family of surface, Comput. Meth. Appl. Mech. Eng. 138 (1996) 213–225.
[6] I.H. Seol, F.L. Litvin, Computerized design, generation and simulation of meshing and contact of worm-gear drives with improved geometry, Comput. Meth. Appl. Mech. Eng. 138 (1996) 73–103.
[7] V. Simon, Characteristics of a new type of cylindrical worm-gear drives, ASME J. Mech. Des. 120 (1998) 139–146.
[8] F.L. Litvin, An analysis of undercut conditions and of appearance of contact lines envelope conditions of gears, ASME J. Mech. Des. 100 (1978) 423–432.
[9] F.L. Litvin, I.H. Seol, D. Kim, J. Lu, A.G. Wang, A. Egelja, X. Zhao, Kinematic and geometric models of gear drives, ASME J. Mech. Des. 118 (1996) 544–550.
[10] J.H. Kuang, Y.T. Yang, A reconsideration of the geometry factor for the standard and profile shifted teeth, ASME J. Mech. Des. 111 (1989) 402–413.
[11] B.W. Bair, C.B. Tsay, ZK-type dual-lead worm and worm gear drives: geometry, ASME J. Mech. Des. 120 (1998) 414–421.
[12] B.W. Bair, C.B. Tsay, ZK-type dual-lead worm and worm gear drives: contact teeth, contact ratios and kinematic errors, ASME J. Mech. Des. 120 (1998) 422–428.
[13] Z.H. Fong, C.B. Tsay, The undercutting of circular-cut spiral bevel gears, ASME J. Mech. Des. 114 (1992) 317–325.
[14] F.L. Litvin, Theory of Gearing, NASA Reference Publication RP-1212, Washington, DC, 1989.
[15] F.L. Litvin, Gear Geometry and Applied Theory, Prentice-Hall, Englewood Cliffs, NJ, 1994.
[16] J.E. Shigley, C.R. Mischke, Mechanical Engineering Design, 5th Edition, McGraw-Hill, New York, 1989.